Elastic Scattering of Protons from Li^6 Nuclei*

J. A. McCray†
California Institute of Technology, Pasadena, California
(Received 31 January 1963)

The differential elastic scattering cross section for protons from Li^6 nuclei has been measured for proton energies from 0.45 to 2.9 MeV at six different angles. The scattering data are consistent with an s- and p-wave phase shift analysis, assuming a single p-wave $\frac{5}{2}^-$ state to be present at about $E_p(\text{lab})=1.84$ MeV, with resonance parameters similar to the parameters previously assigned to the corresponding level in Li^7, and a very broad s-wave $\frac{1}{2}^+$ state at higher energy. It is also possible to fit the scattering and reaction data with a p-wave $\frac{3}{2}^-$ state and a different choice of s-wave background. A p-wave $\frac{1}{2}^-$ state is not consistent with the data. No evidence has been found for the existence of a previously reported $\frac{3}{2}^+$ state near $E_p(\text{lab})=1$ MeV. Removal of the simplifying assumption that only one p-wave state is participating would probably lead to different conclusions about the nature of the s-wave scattering. The relative stopping cross section for protons in lithium was also measured and found to follow the Bloch formula from 0.8 to 2.8 MeV.

I. INTRODUCTION

THE mirror nuclei Li^7 and Be^7 have been the objects of many studies.[1,2] The first three levels of Be^7 have been well established experimentally, but the region between 6 and 8 MeV has not been fully studied. This region in Be^7 corresponds to proton energies of 0.45 to 2.9 MeV. The only reactions which need to be considered in this energy range are the elastic scattering of protons, the (p,α) reaction, and radiative capture of protons. Bashkin and Richards[3] measured the elastic scattering of protons from Li^6 at one back angle with a natural Li target over the range of proton energies from 1 to 3 MeV and found a large scattering anomaly at about 1.85 MeV. Recently, Harrison and Whitehead[4] have studied the region in Be^7 from 8 to 15 MeV excitation by bombarding Li^6 with protons and have found a very broad anomaly in the scattering cross section in the region which corresponds to a proton energy of 4 to 5 MeV.

The reaction $Li^6(p,\alpha)He^3$ has been studied by several investigators,[3,5] and all have found a broad resonance at about 1.85 MeV and evidence for some broad structure at lower energies. There is, however, some confusion as to the absolute value of the cross section, although all investigators obtain values for the cross section at about 1 MeV in the region 50 to 150 mb. Marion *et al.*[5] measured angular distributions for this reaction and found large $\cos\theta$ terms which indicate the presence of two compound nuclear states of opposite parity. They assumed the 1.85-MeV resonance to be formed by p-wave protons since they did not have to consider terms higher than $\cos^2\theta$ in their angular distribution. From the integrated cross section they were able to fit the 1.85-MeV resonance with a single-level Breit-Wigner curve assuming $J^\pi=\frac{5}{2}^-$ for the state. With this assignment for the 1.85-MeV resonance, the other interfering state would then have even parity; and if formed by s-wave protons, would have to be $\frac{3}{2}^+$, since a $\frac{5}{2}^-$ p-wave state can only be formed in the $\frac{3}{2}$ spin channel.

The radiative capture of protons has been studied up to 0.75 MeV by Bashkin and Carlson[6] and Warren *et al.*,[7] and has been found to have a cross section of about 10^{-4} mb. Gamma rays were observed to the ground state and to the first excited state of Be^7, and the angular distributions obtained indicated that, if the process occurred through a compound state, the state would have to have odd parity. McCray and Smith[8] have also looked at the radiative capture of protons by Li^6 at higher energies (1 MeV to 2 MeV) and have found large $\cos^2\theta$ terms in the angular distributions. However, the γ-ray yield increases with energy without exhibiting resonant behavior.

II. EXPERIMENTAL APPARATUS AND TECHNIQUE

This experiment was performed in two parts. The low-energy work from 0.45 to 1.2 MeV involved the use of the 2-MV Van de Graaff accelerator, 80° electrostatic analyzer, 2.5-in. scattering chamber, 10.5-in. magnetic spectrometer and cesium iodide scintillation counter, all of which have been previously described.[9–12] The work from 1.0 to 2.9 MeV was accomplished with the use of the 3-MV Van de Graaff

* Research supported by the Office of Naval Research and the U. S. Atomic Energy Commission.
† Present address: University of California, Davis, California.
[1] A. B. Brown, C. W. Snyder, W. A. Fowler, and C. C. Lauritsen, Phys. Rev. **82**, 159 (1951).
[2] F. Ajzenberg-Selove and T. Lauritsen, Nucl. Phys. **11**, 1 (1959).
[3] S. Bashkin and H. T. Richards, Phys. Rev. **84**, 1124 (1951).
[4] W. D. Harrison and A. B. Whitehead, Bull. Am. Phys. Soc. **6**, 505 (1961).
[5] J. B. Marion, G. Weber, and F. S. Mozer, Phys. Rev. **104**, 1402 (1956).
[6] S. Bashkin and R. R. Carlson, Phys. Rev. **97**, 1245 (1955).
[7] J. B. Warren, T. K. Alexander, and G. B. Chadwick, Phys. Rev. **101**, 242 (1956).
[8] J. A. McCray and P. Smith (unpublished).
[9] C. C. Lauritsen, T. Lauritsen, and W. A. Fowler, Phys. Rev. **59**, 241 (1941).
[10] W. A. Fowler, C. C. Lauritsen, and T. Lauritsen, Rev. Sci. Instr. **18**, 818 (1947).
[11] C. W. Snyder, S. Rubin, W. A. Fowler, and C. C. Lauritsen, Rev. Sci. Instr. **21**, 852 (1950).
[12] F. S. Mozer, Ph.D. Thesis, California Institute of Technology, 1956 (unpublished); and F. S. Mozer, Phys. Rev. **104**, 1386 (1956).

accelerator, 90° electrostatic analyzer, 6-in. scattering chamber, 16-in. magnetic spectrometer, and a cesium iodide scintillation counter like the one above. An energy calibration of the 80° electrostatic analyzer was made at the beginning and end of the first part of the experiment with the 872.5-keV resonance[13] in the $F^{19}(p,\alpha\gamma)O^{16}$ reaction. The calibrations agreed to within one part in a thousand. The 90° electrostatic analyzer was calibrated at various times during the high-energy part of the experiment, using the $Li^7(p,n)Be^7$ threshold.[13] Again agreement to within 1/1000 was found. Energy calibrations for the 10.5-in. and the 16-in. magnetic spectrometers were made by scattering protons from clean copper surfaces.

The scattering and reaction cross sections were measured and calculated by using the thick-target method.[14,15] In this method protons of a fixed energy are scattered from a thick Li^6 target into the spectrometer which is set at some angle θ with respect to the incident beam. The number of particles as a function of fluxmeter current is plotted on a diagram known as a spectrometer profile[1] (Fig. 1). The energy of the particles varies inversely as the square of the fluxmeter current. The yield at the top of the profile is related to the cross section and may be calculated if the stopping cross section of protons in lithium is known.

Since there was some doubt about the previously

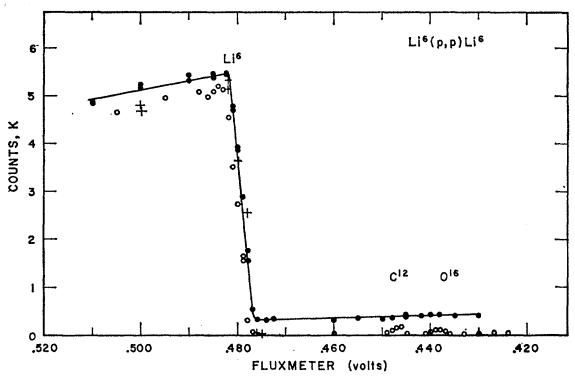

FIG. 1. Spectrometer profile of lithium target. This profile was taken with the 16-in. spectrometer and a Li^6 target in the 6-in. scattering chamber. The solid dots represent the profile taken just after the target was made and show very little indication of C^{12} and O^{16} contamination. When a foil which is thick enough to stop He^{4++} and He^{3++} ions but not protons is placed in front of the detector, the profile indicated by the crosses is found. This observation is taken as evidence that the background consists mainly of He^{4++} and He^{3++} ions. The profile represented by the circles was taken 24 h later with the same target and stopping foil, and shows only a slight contamination with carbon and oxygen. Under bombardment, however, oxygen and carbon collected on the target much more rapidly. The incident laboratory proton energy was about 2.3 MeV and the laboratory angle 81°13′.

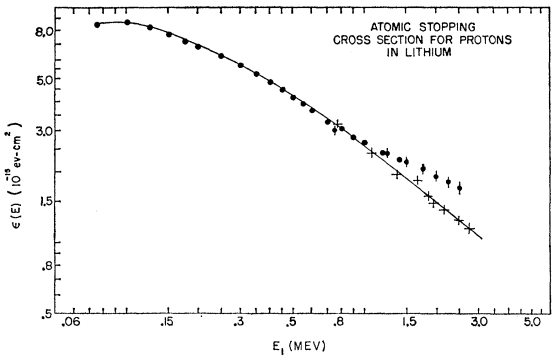

FIG. 2. Atomic stopping cross section for protons in Li. The solid points are measurements of Bader *et al.* (reference 18), and Warters (reference 19) of the stopping cross section for protons in Li. The solid points with vertical bars are determined from the α-particle measurements of Rosenblum (reference 17). The solid curve is the Bloch curve taken from Whaling (reference 16). Relative stopping power measurements made in this experiment are indicated by the crosses.

measured stopping cross section of protons in lithium[16,17] for $E_p > 1$ MeV, a determination of the relative stopping cross sections at several energies was made by scattering protons first from a clean copper target and then from a copper target upon which a thin layer of lithium had been deposited. The results are shown in Fig. 2 and indicate an energy dependence in agreement with the Bloch formula. The relative measurements for $E_p = 0.8 - 2.8$ MeV were normalized to the absolute stopping cross-section measurements of Bader *et al.*,[18] and Warters[19] for $E_p < 1$ MeV. All scattering and reaction cross sections have been normalized to the assumed Rutherford cross section for the elastic scattering of protons by copper.

There are three corrections which must be made in this experiment in order to obtain the yield. The first of these is a background subtraction. For this experiment the major background consisted either of protons scattered from the Li^7 contamination in the target or of doubly charged He^4 and He^3 ions from the reaction $Li^6(p,\alpha)He^3$. A second correction to be made is the loss due to high counting rate. With a dead time of about 10 μsec, this correction was appreciable only for the copper calibration runs and the forward angle Li^6 yields. A third correction arises from charge exchange. Some of the protons, α particles, or He^3 particles, which scatter or are produced within the target, will pick up electrons on the way out and thus will not be observed in the magnetic spectrometer. Allison[20] has measured the probability of this process as a function of energy

[13] J. B. Marion, Rev. Mod. Phys. **33**, 139 (1961).
[14] K. Bardin, Ph. D. Thesis, California Institute of Technology, 1961 (unpublished).
[15] J. A. McCray, Ph.D. Thesis, California Institute of Technology, 1962 (unpublished).
[16] W. Whaling, in *Handbuch der Physik*, edited by S. Flügge (Springer-Verlag, Berlin, 1958), Vol. 34, p. 193.
[17] S. Rosenblum, Ann. Phys. **10**, 408 (1928).
[18] M. Bader, R. E. Pixley, F. S. Mozer, and W. Whaling, Phys. Rev. **103**, 32 (1956).
[19] W. D. Warters, Ph. D. Thesis, California Institute of Technology, 1953 (unpublished).
[20] S. K. Allison, Rev. Mod. Phys. **30**, 1137 (1958).

and gives data for various solids. In the present experiment corrections for this effect were less than 1% for proton scattering but were slightly larger for the $Li^6(p,\alpha)He^3$ reaction.

Since Li forms Li_2O and LiOH very rapidly in air, it is necessary to perform the actual evaporation for the lithium target somewhere in the scattering chamber. The targets must be smooth and they must not deteriorate too quickly under particle bombardment. Freshly evaporated copper on a clean microscope slide was found to be a very satisfactory backing material for the Li targets. The microscope slides provided the smoothness and the copper provided enough thermal conductivity to prevent deterioration by local heating. The copper evaporation was performed in a vacuum bell jar and the copper blanks then placed immediately in the scattering chamber. A furnace was situated below each scattering chamber so that with the use of a long target rod, the Li evaporations could be carried out and the targets moved directly up into the scattering chamber. Two Li^6 metal samples were used, one of 94.5% purity and the other of 99.7% purity. Most of the work was done with the higher purity sample. The Li^6 metal was cleaned under kerosene, then transferred directly to the furnace and the system placed under vacuum. The furnace consisted of a carbon rod heated by a molybdenum coil. A cold trap was placed between the furnace area and the target area in the target chamber.

The cross section for the elastic scattering of protons from Li^6 nuclei was measured from about 0.45 to 2.9 MeV at intervals of 12.5 or 20 keV for c.m. angles near the zeros of the first and second Legendre polynomials and near the farthest back angle obtainable ($\approx 160°$). A sample of the results obtained is shown in Fig. 3 and indicates that the scattering cross section follows the Rutherford formula near 0.45 MeV and that $\sigma_{\text{scattering}}/\sigma_{\text{Rutherford}}$ rises gradually up to about 1.1 MeV, where it then exhibits resonant behavior up to about 3 MeV. For more detailed results the reader should see reference 15. The variation of the cross section as a function of angle from the backward angles to 90° suggests that the resonance might be formed by odd l-wave protons. The cross section measured at 90° will then be the most informative, since the interference terms will vanish; this is shown in Fig. 4. A comparison of the 160° data ($\theta_L \approx 156°$) with that of Bashkin and Richards[3] at $\theta_L \approx 164°$ indicates that their cross sections are about 2/3 of the values measured in the present experiment. It is apparent that no prominent anomaly occurs in the region of 1 MeV. Thus, any resonant state in this region must have a small value of Γ_p/Γ. The scattering cross section was also measured at c.m. angles near 140°, 110°, and 70° at intervals of 100 keV. Figures 5 though 7 show some of the 25 angular distributions obtained. The error bars indicate relative errors which are 3% for the backward angles and 4% for the 70° and 90° data.

In order to analyze the scattering data it is necessary to know the $Li^6(p,\alpha)He^3$ reaction cross section. Since the reported values[2,3,5] for this reaction varied by a factor of 3, a new determination was deemed necessary. The thick-target method was used and the angle of the spectrometer set at $\theta_L = 95°45'$ to detect the He^3's which correspond to the α's at $\theta_L = 60°$ measured by Marion *et al.*[5] The cross sections obtained were found to be about 55% of the values quoted by Marion *et al.*[5] but were in agreement with those of Burcham and Freeman.[21] The relative cross sections measured by Marion *et al.*[5] were assumed to be correct and normalized to 55% of the quoted absolute values.

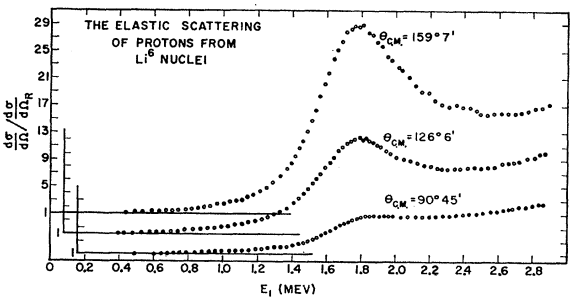

FIG. 3. Excitation function for $Li^6(p,p)Li^6$. The ratio of the measured elastic scattering cross section to the cross section for Rutherford scattering from a point charge is plotted as a function of laboratory proton energy (in MeV) for three angles corresponding approximately to zeros of the first and second Legendre polynomials and the farthest back angle obtainable.

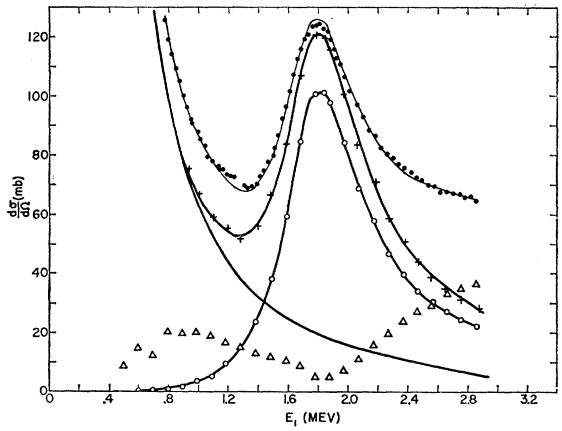

FIG. 4. Scattering cross section for $Li^6(p,p)Li^6$ at $\theta_{c.m.} = 90°$. The measured cross section is indicated by the solid dots. The solid curve represents the calculated Rutherford cross section. The curve indicated by the open circles is that calculated for a $5/2^-$ p-wave resonant state as indicated in the text. The curve designated by crosses is the sum of the Rutherford cross section and the cross section due to the $5/2^-$ p-wave resonant state. The triangles represent the s-wave scattering cross section calculated from the s-wave scattering amplitudes which were determined in the scattering analysis of the data. The solid curve through the experimental points is the sum of the s-wave background, the $5/2^-$ p-wave resonant state, and the Rutherford cross section.

[21] W. E. Burcham and J. M. Freeman, Phil. Mag. **41**, 921 (1950).

The probable error in the absolute values of the measured scattering cross sections was estimated to be about 5%.

III. THEORETICAL ANALYSIS OF THE DATA

The method of analysis used here is essentially that described by Christy[22] and Mozer.[12] For a particular incident particle and target nucleus the amplitude matrix elements are worked out for the lowest orbital angular momentum waves which are thought to contribute to the scattering. For the case of $Li^6(p,p)$ Li^6 it is a reasonable assumption that over the energy region investigated in this experiment only s- and p-wave protons interact appreciably with the Li^6 nucleus. For this case then, one must combine a proton of spin and parity $\frac{1}{2}^+$ with a Li^6 nucleus of spin and parity 1^+. Thus, there are two possible channel spins, $\frac{1}{2}^+$ and $\frac{3}{2}^+$. If one considers only s waves, nuclear states in Be^7 may be formed which have total spins and parities of $J^\pi=\frac{1}{2}^+$ or $\frac{3}{2}^+$. Since the angular momentum and parity associated with p waves is 1^-, nuclear states may be formed through the $\frac{1}{2}$ spin channel which have $J^\pi=\frac{1}{2}^-$ and $\frac{3}{2}^-$; the states which may be formed through the $\frac{3}{2}$ spin channel have $J^\pi=\frac{1}{2}^-$, $\frac{3}{2}^-$, and $\frac{5}{2}^-$.

The experimental data indicate the presence of a strong resonance in the vicinity of 1.85 MeV. The angular distributions show a decrease in cross section from backward angles to $\theta_{c.m.}=90°$. If only s and p waves are assumed to be important in this energy region, then this nuclear resonance would have to be formed by p waves. (The reduced proton width calculated by assuming f waves exceeds the single-particle limit.) The spin and parity of this state then must be $\frac{1}{2}^-$, $\frac{3}{2}^-$, or $\frac{5}{2}^-$.

The mirror nuclei[2] Li^7 and Be^7 have corresponding levels for the first and second excited states. There is also a well-defined state at 7.47 MeV in Li^7 which probably corresponds to the resonance seen in Be^7 at 7.18 MeV. From the total absorption cross section for neutrons on Li^6 and the cross section for the reaction $Li^6(n,\alpha)H^3$, the spin of the above state in Li^7 was found to be $\frac{5}{2}^-$.[23] It was not possible because of the divergent scattering cross section at forward angles and the unknown s-wave background, to perform a similar analysis in the case of $Li^6(p,p)Li^6$ and $Li^6(p,\alpha)He^3$. However, it seemed reasonable to assume that the state in Be^7 at 7.18 MeV is the mirror state of the $\frac{5}{2}^-$ state in Li^7; therefore, an analysis was performed for the $Li^6(p,p)Li^6$ scattering under the assumption that only s and p waves contribute and that the p-wave scattering is only through a $\frac{5}{2}^-$ resonant state. If these assumptions are made, there are three unknown complex amplitudes which describe the scattering, one for the resonant

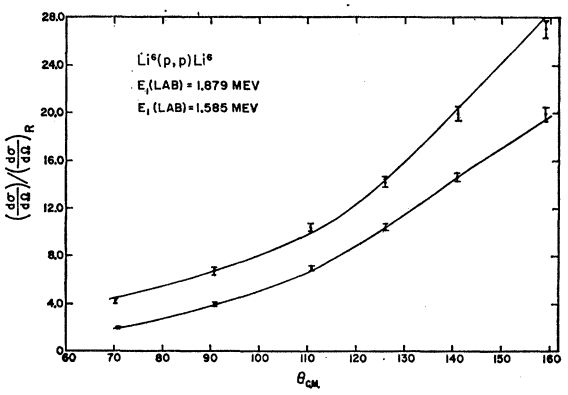

FIG. 6. The elastic scattering of protons from Li^6 nuclei at $E_1=1.585$ MeV is represented by the upper curve and at $E_1=1.879$ MeV by the lower curve. The solid lines are the theoretical fits for a $5/2^-$ p-wave state resonant at $E_p=1.84$ MeV plus s-wave background.

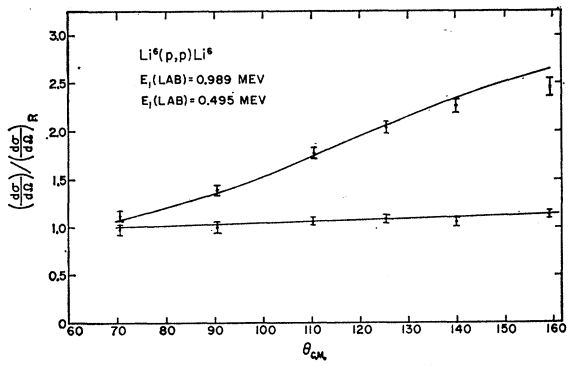

FIG. 5. The elastic scattering of protons from Li^6 nuclei at $E_1=0.495$ MeV is represented by the upper curve and at $E_1=0.989$ MeV by the lower curve. The solid lines are the theoretical fits for a $5/2^-$ p-wave state resonant at $E_p=1.84$ MeV plus s-wave background.

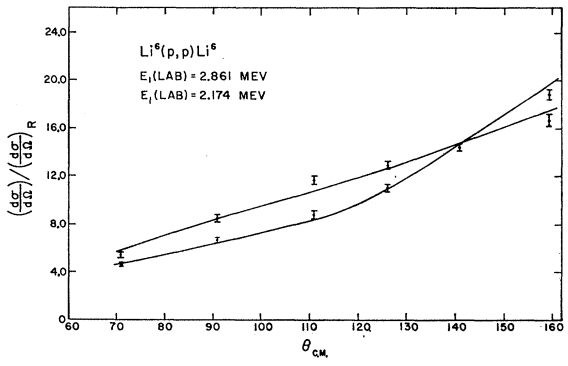

FIG. 7. The elastic scattering of protons from Li^6 nuclei at $E_1=2.174$ MeV is represented by the upper curve and at $E_1=2.861$ MeV by the lower curve. The solid lines are the theoretical fits for a $5/2^-$ p-wave state resonant at $E_p=1.84$ MeV plus s-wave background.

[22] R. F. Christy, Physica **22**, 1009 (1956).

[23] C. H. Johnson, H. B. Willard, and J. K. Bair, Phys. Rev. **96**, 985 (1954).

p-wave state, and two for the s-wave scattering, one for each spin channel. The real and imaginary parts of these complex amplitudes are written as follows:

$$\begin{aligned} f_{sc}(5/2)&=f(5/2)+ig(5/2)-1,\\ f_{sc}(1/2)&=f(1/2)+ig(1/2)-1,\\ f_{sc}(3/2)&=f(3/2)+ig(3/2)-1. \end{aligned} \tag{1}$$

It is convenient to define the real quantities X, Y, and U in terms of the last two s-wave amplitudes above:

$$\begin{aligned} X&=1/3f(1/2)+2/3f(3/2),\\ Y&=1/3g(1/2)+2/3g(3/2), \end{aligned} \tag{2}$$

$$U=1-1/3[f^2(1/2)+g^2(1/2)]-2/3[f^2(3/2)+g^2(3/2)]. \tag{3}$$

The parameter U is related to the s-wave reaction cross section in the following way:

$$U=k^2\sigma_R(s\text{-wave})/\pi. \tag{4}$$

Under the above assumptions the differential cross section for scattering is found to be[22]

$$\begin{aligned} \frac{d\sigma}{d\Omega}(\theta,E)=&\left[R+\left(\frac{\sqrt{R}}{k}\sin\xi-\frac{1}{2k^2}\right)(X-1)-\left(\frac{\sqrt{R}}{k}\cos\xi\right)Y-\frac{U}{4k^2}\right]+\frac{1}{2k^2}\{(f(3/2)-1)[(f(5/2)-1)\cos2\eta_1\\ &-g(5/2)\sin2\eta_1]+g(3/2)[(f(5/2)-1)\sin2\eta_1+g(5/2)\cos2\eta_1]\}\cos\theta-\frac{\sqrt{R}}{k}\{(f(5/2)-1)\sin[2\eta_1-\xi]\\ &+g(5/2)\cos[2\eta_1-\xi]\}\cos\theta+\frac{9}{50k^2}[1+(7/6)\cos^2\theta][(f(5/2)-1)^2+g^2(5/2)], \end{aligned} \tag{5}$$

where R is the Rutherford cross section, ξ is the phase of the Rutherford amplitude, k is the p-Li^6 channel wave number, and $\eta_1=\tan^{-1}(3e^2/\hbar v)$ is the Coulomb phase shift with v equal to the relative velocity for the p-Li^6 channel. The first term above is the s-wave+Rutherford interference scattering in the form given by Christy. The second term (on two lines) is the s-wave, p-wave interference term. The third term (also on two lines) is the p-wave, Rutherford interference term, and the fourth term is the pure resonance contribution of the $\frac{5}{2}^-$ p-wave state.

The object of the analysis is to find a set of six coefficients, $f(1/2)$, $g(1/2)$, $f(3/2)$, $g(3/2)$, $f(5/2)$, $g(5/2)$, as functions of energy which describe the 25 angular distributions over the energy region considered. These coefficients must, however, also be consistent with the reaction data for $Li^6(p,\alpha)He^3$ and they must vary smoothly as a function of energy.

Equation (5) may be written in terms of X and Y as a straight line.

$$Y=A(\theta)X+C(\theta). \tag{6}$$

The slopes of these lines are exactly the same as those found for the s-wave case.

$$A(\theta)=\frac{(\sin\xi)-1/2k\sqrt{R}}{\cos\xi}. \tag{7}$$

The intercepts, however, contain an additional term besides the s-wave intercept $B(\theta)$.

$$C(\theta)=B(\theta)+D(\theta), \tag{8}$$

where

$$B(\theta)=\left\{k\sqrt{R}-\sin\xi+\frac{1}{k\sqrt{R}}\left[\frac{1}{2}-k^2\left(\frac{\sigma_R}{4\pi}+\frac{d\sigma}{d\Omega}(\theta)\right)\right]\right\}\Big/\cos\xi. \tag{9}$$

The additional term may be broken up into two parts, the resonance p-wave contribution plus p-wave-Rutherford interference term $H(\theta)$, and the s-wave, p-wave interference term $ZG(\theta)$. Since the $\frac{5}{2}^-$ p-wave state is formed only through the $\frac{3}{2}$ spin channel, the latter term contains only the s-wave $\frac{3}{2}$ spin channel amplitude. The term Z is used to make the final fit to the scattering data and, hence, provides the additional information necessary to separate the four unknown s-wave parameters. This is given in the form of a straight line for $g(3/2)$ in terms of $f(3/2)$.

$$g(3/2)=-Sf(3/2)+(S+Z), \tag{10}$$

where S is a function of the $\frac{5}{2}^-$ p-wave parameters. The quantities $f(1/2)$ and $g(1/2)$ may be eliminated from Eqs. (2) and (3) to give a second relation involving $f(3/2)$ and $g(3/2)$ which is a circle.

$$[f(3/2)-X]^2+[g(3/2)-Y]^2=\tfrac{1}{2}[(1-U)-(X^2+Y^2)]. \tag{11}$$

Thus, if X, Y, U, and Z may be determined from the experimental data, the above two equations provide two solutions if the straight line intersects the circle. A choice may be made between the two solutions by invoking conservation of particles and continuity of nuclear amplitudes as a function of energy.

In order to perform the above analysis, assumptions must be made about the resonance parameters of the $\frac{5}{2}^-$ p-wave state. If reasonable straight-line extrapolations are made for the s-wave $Li^6(p,\alpha)He^3$ reaction cross section, reduced proton and alpha widths may be derived from the cross section at resonance. The values found were very close to those determined by Gabbard[24] for the mirror state in Li^7. The resonant energy was determined from the scattering data at 90° (Fig. 4).

[24] F. Gabbard (private communication to F. Ajzenberg-Selove).

The $Li^6(p,\alpha)He^3$ integrated reaction cross section for p-wave protons through a state of spin and parity $\frac{5}{2}^-$ was, then, computed and subtracted from the measured cross section in order to find a better approximation for the s-wave background parameter U as a function of energy. The p-wave contributions to the scattering were also computed using penetration factors[25] and level shifts.[26]

An s-wave fit was possible at low energies (Fig. 8), but at higher energies (Fig. 9) no intersection was found for the six lines when only the s-wave intercepts were computed. The effect of adding the $H(\theta)$ intercepts is also shown in Fig. 9. The parameter Z was chosen in order to bring the six lines to an intersection within the experimental errors (Fig. 10). A solution for the s-wave scattering amplitudes was then found from Eqs. (10) and (11). This procedure was then used, beginning at low energies and continuing to higher energies, to determine an acceptable set of s-wave parameters $f(1/2)$, $g(1/2)$, $f(3/2)$, and $g(3/2)$. The resulting complex points are shown in Fig. 11 along with the parameters X, Y and $f(5/2)$, $g(5/2)$. At each energy these six values for $f(1/2)$, $5(1/2)$, $f(3/2)$, $g(3/2)$, $f(5/2)$, $g(5/2)$ were substituted into Eq. (5) for each of the six angles and values of $(d\sigma/d\Omega)/R$ obtained. The solid curves drawn on each angular distribution represent the results of these calculations. Given the set of s-wave parameters as a function of energy it was then possible to calculate the s-wave scattering cross section at 90° as a function of energy and to add this contribution to the sum of the Rutherford scattering cross section and the resonance p-wave scattering cross

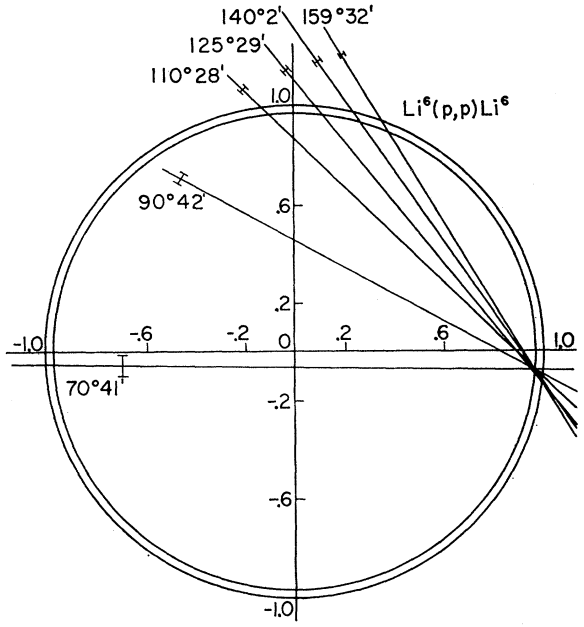

FIG. 8. S-wave scattering amplitude diagram at $E_1=0.692$ MeV. The equation $Y=A(\theta)X+B(\theta)$, where $B(\theta)$ is the s-wave intercept, is plotted in the complex plane for the six c.m. angles used in the experiment. At this low energy the six lines come to an intersection within the experimental relative errors. The complex point (X,Y) must be the same for all angles at a given energy and must fall within the inner circle with radius equal to $(1-U)^{1/2}$.

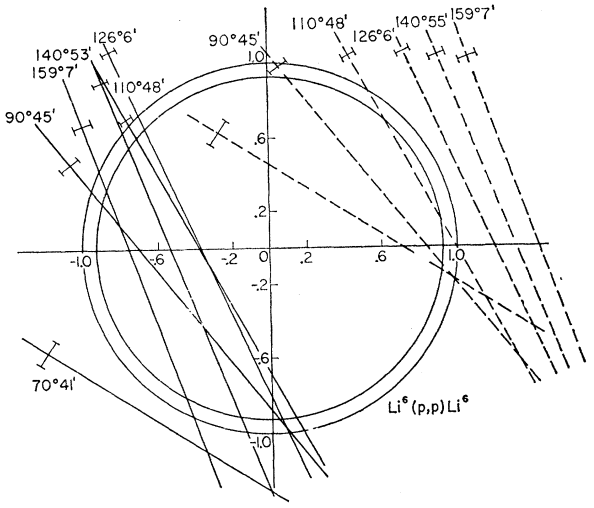

FIG. 9. S-wave scattering amplitude diagram at $E_1=1.879$ MeV. The six lines at this energy do not intersect and indicate that the resonant structure at this energy cannot be described by s waves alone. The dashed lines represent the addition of the $H(\theta)$ intercepts to the $B(\theta)$ intercepts. Since an intersection is still not possible, the s-wave, p-wave interference intercept $ZG(\theta)$ must be computed for each angle.

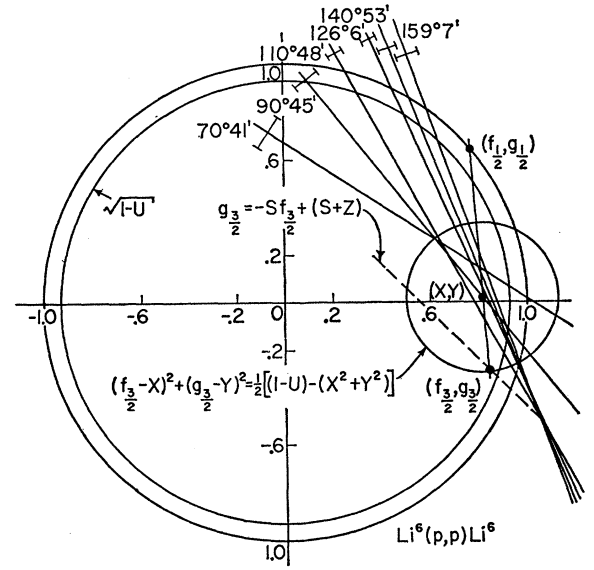

FIG. 10. S-wave scattering amplitude diagram at $E_1=1.879$ MeV. In this diagram the six lines $Y=A(\theta)X+C(\theta)$ are plotted where $C(\theta)$ is the s-plus p-wave intercept.

[25] W. T. Sharp, H. E. Gove and E. B. Paul, A.E.C.L. Report No. 268, Chalk River, Ontario, 1955 (unpublished).
[26] R. G. Thomas, Phys. Rev. **81**, 148 (1951).

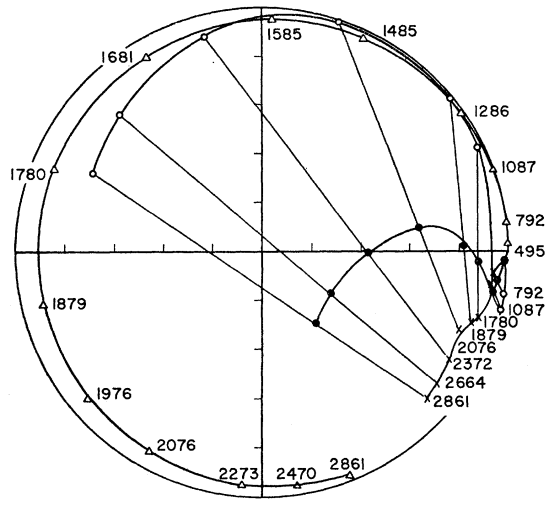

FIG. 11. Scattering amplitude diagram. This figure represents the region in the complex plane within the unit circle. For the case of $Li^6(p,p)Li^6$ the scattering cross section may be written in terms of three complex scattering amplitudes. The assumption is made that only s and p waves contribute and that the p-wave scattering is through a single resonant $5/2^-$ state. The energy variations of the complex scattering amplitudes for this state $[f(5/2), g(5/2)]$, for s-wave scattering through the 3/2 spin channel $[f(3/2, g(3/2)]$, and for s-wave scattering through the 1/2 spin channel $[f(1/2), g(1/2)]$ are indicated in the diagram. The energy variation of a fourth complex amplitude (X,Y), defined in the text, is also shown in the figure. The curves are labeled as follows: s-wave (X,Y) amplitude, ●; s-wave 1/2 spin channel amplitude, ○; s-wave 3/2 spin channel amplitude, ×; p-wave 5/2 resonant amplitude, △.

section to give the scattering cross sections predicted by Eq. (5) at this angle. The result is shown in Fig. 4 and appears to be a resonable fit to the measured scattering cross section.

Consideration must also be given to the possibility of $\frac{1}{2}^-$ and $\frac{3}{2}^-$ assignments for the 1.84-MeV p-wave resonance. If the single p-wave resonance assumed in the analysis has the assignment $J^\pi=\frac{1}{2}^-$ or $\frac{3}{2}^-$, the state may be formed through either spin channel and a channel spin mixing parameter must be introduced. The scattering amplitude for the $\frac{1}{2}^-$ assignment then becomes

$$f_{sc}(1/2^-)=\alpha_i\alpha_j[f(1/2^-)+ig(1/2^-)-1], \quad i,j=1/2 \text{ or } 3/2, \quad (12)$$

where $\alpha_{1/2}^2$ is the probability of forming the $\frac{1}{2}^-$ p-wave state through the 1/2 spin channel and $\alpha_{3/2}^2$ is the probability of forming the $\frac{1}{2}^-$ p-wave state through the 3/2 spin channel. Since the α_i^2 are probabilities and there are only two spin channels, the following relation must hold

$$\alpha^2(1/2)+\alpha^2(3/2)=1. \quad (13)$$

Since there is only one additional quantity involved, one may speak of a channel spin mixing parameter M which is defined here to be equal to $\alpha^2(1/2)$.

The scattering cross section is then found from the amplitude matrix in the same way as that described for the case of $J^\pi=\frac{5}{2}^-$. All of the terms for a $J^\pi=\frac{1}{2}^-$ p-wave state must be considered including the channel spin flip terms (i.e., scattering events which involve a change of channel spin). The correctness of the p-wave resonant term in the cross section may be checked by integrating the cross section over solid angle. The interference terms drop out and the result must agree with the Breit-Wigner formula at resonance,

$$\sigma_{\text{scatt}}(\text{res.})=\frac{2J+1}{6}\frac{4\pi}{k^2}\left(\frac{\Gamma_p}{\Gamma}\right)^2. \quad (14)$$

The scattering cross section for a single $J^\pi=\frac{1}{2}^-$ p-wave resonant state is found to be

$$\frac{d\sigma}{d\Omega}(\theta,E)=R+\left(\frac{\sqrt{R}}{k}\sin\xi-\frac{1}{2k^2}\right)(X-1)-\left(\frac{\sqrt{R}}{k}\cos\xi\right)Y-\frac{U}{4k^2}+\frac{1}{3}\left(\frac{Z}{2k^2}\right)\{[f(1/2^-)-1]\sin2\eta_1+g(1/2^-)\cos2\eta_1\}\cos\theta$$
$$-\frac{1}{3}\frac{\sqrt{R}}{k}\{[f(1/2^-)-1]\sin[2\eta_1-\xi]+g(1/2^-)\cos[2\eta_1-\xi]\}\cos\theta+\frac{1}{12k^2}\{[f(1/2^-)-1]^2+g^2(1/2^-)\}. \quad (15)$$

The coefficient Z is defined similarly to Eq. (10) but now

$$g(3/2)=-Sf(3/2)+[Z+S-3M(SX+Y)]/(1-3M). \quad (16)$$

This equation combined with the circle equation (11) must then yield an acceptable solution for the s-wave scattering if this choice of J^π is correct. The p-wave resonance parameters may be found from the $Li^6(p,\alpha)He^3$ reaction cross section by the procedure outlined above. An s-wave background was chosen which was similar to that used for the $J^\pi=\frac{5}{2}^-$ case.

With the assumption that only s- and p-wave contributions are present, the assignment $J^\pi=\frac{1}{2}^-$ is excluded by the experimental data. This is primarily due to the fact that the p-wave pure resonance term is isotropic for $J=1/2$, and this restriction makes it impossible to fit the observed angular distributions.

The analysis in terms of a $\frac{3}{2}^-$ p-wave state proceeds in exactly the same manner as that for the $\frac{1}{2}^-$ case. The scattering amplitude is given by

$$f_{sc}(3/2^-)=\alpha_i\alpha_j[f(3/2^-)+ig(3/2^-)-1], \quad i,j=1/2 \text{ or } 3/2. \quad (17)$$

The channel spin mixing parameter M may be defined in the same way as above. The scattering cross section

then becomes

$$\frac{d\sigma}{d\Omega}(\theta,E)=R+\left(\frac{\sqrt{R}}{k}\sin\xi-\frac{1}{2k^2}\right)(X-1)-\left(\frac{\sqrt{R}}{k}\cos\xi\right)Y-\frac{U}{4k^2}+\frac{2}{3}\left(\frac{Z}{2k^2}\right)\{[f(3/2^-)-1]\sin 2\eta_1$$
$$+g(3/2^-)\cos 2\eta_1\}\cos\theta-\frac{2}{3}\frac{\sqrt{R}}{k}\{[f(3/2^-)-1]\sin[2\eta_1-\xi]+g(3/2^-)\cos[2\eta_1-\xi]\}\cos\theta$$
$$+\frac{1}{300k^2}[\beta+3(50-\beta)\cos^2\theta]\{[f(3/2^-)-1]^2+g^2(3/2^-)\},\quad(18)$$

where

$$\beta=34+72M-81M^2 \quad (19)$$

and Z is defined as in Eq. (16).

Various values of channel spin mixing parameter M were chosen and an analysis carried out in the same manner as for the $\frac{5}{2}^-$ case and the $\frac{1}{2}^-$ case. The case of $M=1/2$ (i.e., if the $\frac{3}{2}^-$ state is formed equally through both spin channels) may be excluded since it gives an almost isotropic p-wave intensity contribution to the scattering. However, for the cases of the $\frac{3}{2}^-$ state being formed almost entirely through either the 1/2 spin channel or the 3/2 spin channel, a fit to the data can be made with a different choice of s-wave background. In these cases the s-wave background does not show resonant behavior in the 1/2 channel spin.

IV. CONCLUSIONS

Over the region studied, Eq. (5) appears to describe the measured elastic scattering cross section. The p-wave scattering is consistent with resonant scattering through a state of spin and parity $J^\pi=\frac{5}{2}^-$ with resonance parameters in agreement with those from the mirror level in Li^7 and with the $Li^6(p,\alpha)He^3$ reaction cross section. A $1/2^-$ assignment for the p-wave resonance is inconsistent with the data. The possibility of a $3/2^-$ assignment for the p-wave state with a different choice in s-wave background, however, cannot be excluded on the grounds of the proton scattering data alone. The s-wave scattering phase shift in the 3/2 spin channel (Fig. 11) does not show a resonance in the region from 0.45 to 2.9 MeV. Hence, if a $3/2^+$ state exists at about 6.35-MeV excitation in the compound nucleus Be^7, it must have a small Γ_p/Γ and a large Γ_α/Γ. This state should then have shown up in the elastic scattering of He^3 from He^4.[27] It should also be noted that the mirror level of this proposed $3/2^+$ state was not excited in the $Li^6(d,p)Li^7$ reaction.[28] This evidence also suggests a small value of Γ_n/Γ for this state. Of possible interest here are the cluster model calculations of Pearlstein *et al.*[29] and Khanna *et al.*[30] who conclude that neither an alpha-particle plus mass-3 cluster, nor a neutron plus Li^6 cluster, will yield a $3/2^+$ state at this energy.

The p-wave $5/2^-$ state at about 7.2-MeV excitation is now usually assigned the designation $^4P_{5/2}$, on an $L-S$ coupling model.[31,32] In addition, these calculations predict a state with designation $^2F_{5/2}$ somewhere in the vicinity of 6-MeV excitation. A $5/2^-$ state in the vicinity of 6 MeV is also predicted on the basis of the unified model.[33] If such a state falls within the region corresponding to 0.45 MeV$<E_p<$1.4 MeV, the present experiment suggests that the state must have a small value of Γ_p/Γ. A resonance has been found in this region by Tombrello *et al.*[27] in the scattering of He^3 by He^4, and a partial wave analysis indicates that it is most likely the $^2F_{5/2}$ state.

The s-wave scattering phase shift in the 1/2 spin channel has qualitatively the same behavior as that in the 3/2 spin channel at low energy, but begins to exhibit resonant behavior at higher energies. This suggests the presence of a broad $1/2^+$ s-wave state in Be^7 at an excitation energy above 8 MeV. It should be

TABLE I. The following resonant parameters for the 1.84-MeV p-wave resonant state in Be^7 are consistent with the measured scattering and reaction data. The channel radii used were $a(p-Li^6)=4.08$ F and $a(He^3-\alpha)=4.39$ F. The resonant parameters given by Gabbard for the mirror state in Li^7 are also listed. The channel radii used by Gabbard were $a(n-Li^6)=3.94$ F and $a(t-\alpha)=4.39$ F.

Nucleus	Be^{7*}	Li^{7*}
J^π	$5/2^-$	$5/2^-$
E_R(lab) (MeV)	1.84	0.262
$\Gamma(E_R)$ (MeV)	0.836	0.154
E_λ (MeV above ground)	7.58	7.70
$\Gamma_{p,n}(E_R)$ (MeV)	0.798	0.118
$\gamma_{p,n}^2$ (MeV-F)	5.02	4.85
$\theta_{p,n}^2$	0.28	0.26
$\Gamma_\alpha(E_R)$ (MeV)	0.038	0.036
γ_α^2 (MeV-F)	0.101	0.101
θ_α^2	0.012	0.012

[27] T. A. Tombrello, P. D. Parker, and C. A. Barnes, Bull. Am. Phys. Soc. **7**, 268 (1962).
[28] E. W. Hamburger and J. R. Cameron, Phys. Rev. **117**, 781 (1960).
[29] L. D. Pearlstein, Y. C. Tang, and K. Wildermuth, Nucl. Phys. **18**, 23 (1960).
[30] F. C. Khanna, Y. C. Tang and K. Wildermuth, Phys. Rev. **124**, 515 (1961).
[31] D. R. Inglis, Rev. Mod. Phys. **25**, 390 (1953).
[32] J. B. Marion, Nucl. Phys. **4**, 282 (1957).
[33] A. B. Clegg, Phil. Mag. **6**, 1207 (1961).

noted, however, that the behavior of the s-wave scattering determined in this analysis is dependent upon the assumption that only one resonant p-wave state is present. The resonant parameters used in the analysis of the p-wave resonant state in Be^7 at an excitation energy of 7.58 MeV are shown in Table I along with the corresponding values for the mirror level in Li^7 as given by Gabbard. (The author wishes to thank Dr. F. Gabbard for permission to use the results of his calculations.)

ACKNOWLEDGMENTS

The author wishes to express his gratitude to Dr. C. A. Barnes for suggesting this work and for his continuous encouragement and discussions concerning it. The interest shown by Dr. W. A. Fowler and Dr. T. Lauritsen was greatly appreciated. The advice given by Dr. R. F. Christy on the theoretical analysis of the data was also very helpful. The author would like to thank Mrs. Barbara Zimmerman for her assistance in performing part of the calculations.

PHYSICAL REVIEW VOLUME 130, NUMBER 5 1 JUNE 1963

New Isomers of Astatine-212

W. BARCLAY JONES
Lawrence Radiation Laboratory, University of California, Berkeley, California
(Received 8 March 1963)

The $_{83}Bi^{209}(\alpha,n)_{85}At^{212}$ reaction was investigated in the energy range of 17 to 25 MeV. Astatine-122 was observed to decay by alpha-particle emission. An alpha decay group of 7.60 and 7.66 MeV having a half-life of 0.305 sec and another group of 7.82 and 7.88 MeV having a half-life of 0.120 sec were observed. Relative excitation functions were obtained for both isomers. An energy-level diagram for the alpha decay of astatine-212 is proposed.

THE $_{83}Bi^{209}(\alpha,n)_{85}At^{212}$ reaction was investigated at the Crocker Laboratory 60-in. cyclotron of the University of California. Previous work on this reaction[1-4] reports that At^{212} has a half-life of 0.20 sec, and emits alpha particles of 7.6 or 7.88 MeV.

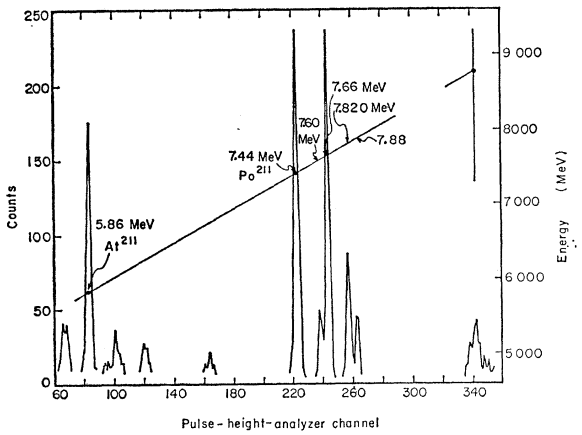

FIG. 1. Spectrum of alpha energies for 24-MeV alpha particles on bismuth.

In this experiment, the alpha decay energies were measured with a phosphorus-diffused-junction counter having an energy resolution of 30 keV. The spectra were observed at selected intervals between cyclotron beam bursts. The spectrum taken at a bombarding energy of 24 MeV is shown in Fig. 1 (the small peaks at 5.63, 6.04, 6.28, 6.78, and 8.78 MeV are due to the calibration source, Th^{228}). The results of the experiment are summarized in Table I. The half-life associated with each of these alpha energies was measured individually by time analysis of each pulse height.

A search was made for a gamma transition between the states responsible for the 7.82- and 7.60-MeV alpha groups by means of detecting the conversion electrons; however, no such transition was observed. Less than 1% of the alpha activity could have a gamma decay in the energy range from 100 to 600 keV; however, a $\approx$63-keV transition was observed with a half-life of $\sim$0.13 sec.[5]

TABLE I. Alpha-decay energies and half-lives for At^{212}.

Alpha decay energy (MeV)	Half-life (sec)	Approximate relative abundance (%)	Hindrance factor
7.60	0.305	20	6200
7.66	0.305	80	1700
7.82	0.120	80	1600
7.88	0.120	20	9500

* Work supported by the U. S. Atomic Energy Commission.
[1] M. Weissbluth, T. M. Putnam, and E. Segrè (unpublished work) reported by D. Strominger, J. M. Hollander, and G. T. Seaborg, Rev. Mod. Phys. **30**, 585 (1958).
[2] M. M. Winn, Proc. Phys. Soc. (London) **A67**, 949 (1954).
[3] J. C. Ritter and W. G. Smith, Phys. Rev. **128**, 1778 (1962).
[4] R. G. Griffioen and R. D. Macfarlane, in Lawrence Radiation Laboratory Report UCRL-10023, 1962 (unpublished).
[5] F. S. Stephens and R. M. Diamond, Lawrence Radiation Laboratory (private communication).